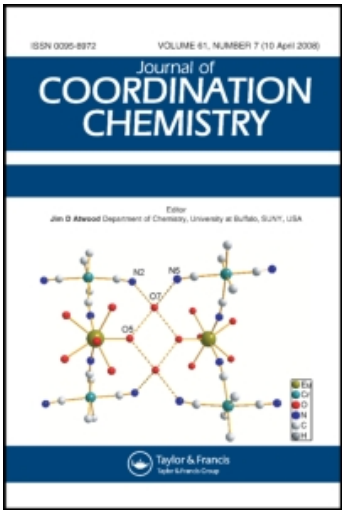

Journal of Coordination Chemistry
Publication details, including instructions for authors and subscription information:
http://www.informaworld.com/smpp/title~content=t713455674

CO and NO complexes of Fe(II) and Co(II) porphyrins

Tatyana E. Shubina[a]; Timothy Clark[a]
[a] Computer-Chemie-Centrum and Interdisciplinary Center for Molecular Materials, Friedrich-Alexander Universität Erlangen-Nürnberg, Nägelsbachstraße 25, 91052 Erlangen, Germany

First published on: 22 July 2010

To cite this Article Shubina, Tatyana E. and Clark, Timothy(2010) 'CO and NO complexes of Fe(II) and Co(II) porphyrins', Journal of Coordination Chemistry, 63: 14, 2854 — 2867, First published on: 22 July 2010 (iFirst)
To link to this Article: DOI: 10.1080/00958972.2010.503346
URL: http://dx.doi.org/10.1080/00958972.2010.503346

Journal of Coordination Chemistry
Vol. 63, Nos. 14–16, 20 July–20 August 2010, 2854–2867

Taylor & Francis
Taylor & Francis Group

CO and NO complexes of Fe(II) and Co(II) porphyrins†

TATYANA E. SHUBINA* and TIMOTHY CLARK*

Computer-Chemie-Centrum and Interdisciplinary Center for Molecular Materials,
Friedrich-Alexander Universität Erlangen-Nürnberg,
Nägelsbachstraße 25, 91052 Erlangen, Germany

(*Received 5 February 2010; in final form 22 April 2010*)

Density functional theory (DFT) calculations on iron(II) (FeP) and cobalt(II) (CoP) porphyrins with nitric oxide (NO) and carbon monoxide (CO) as axial ligands have been performed using BLYP, B3LYP, OLYP, B3PW91, and M06L functionals with double- and triple-ξ basis sets. Optimized geometries and binding energies were found to depend very strongly on the functional and basis set used. MP2 fails completely to describe geometries and binding energies of FeP–CO, CoP–CO, and CoP–NO complexes, but performs relatively well for the FeP–NO complex. The calculated binding energies range from -4.5 to $-19.6\,\mathrm{kcal\,mol^{-1}}$ for CoP–CO, $+4.0$ to $-29.1\,\mathrm{kcal\,mol^{-1}}$ for FeP–CO, $+7.6$ to $-41.1\,\mathrm{kcal\,mol^{-1}}$ for FeP–NO, and -2.2 to $-36.7\,\mathrm{kcal\,mol^{-1}}$ for CoP–NO. B3PW91/6–311 + G(d,p) and OLYP/6–311+G(d,p) perform better than the other functional/basis set combinations in reproducing the available experimental data. A complete active space self-consistent field/complete active space with second-order perturbation theory (CASSCF/CASPT2) analysis of the CO and NO interactions with FeP and CoP can be interpreted either in terms of σ-donation/π-back-donation mechanism (FeP–CO and CoP–CO) or σ bond formation between the $3d_{z^2}$ orbital of metal and the π^* orbital of NO.

Keywords: Metalloporphyrins; Nitric oxide; Carbon monoxide; DFT; MP2

1. Introduction

Metalloporphyrins (MPs) are important in biological systems for oxygen storage and transfer [1], metabolism [2, 3], photosynthesis [4], and quite generally as natural redox reagents and small-molecule storage and transport agents. The use of MPs as acceptor molecules in chemical sensors has long interested researchers [5]. Their rich coordination chemistry can be used in chemical-sensor applications by detecting changes induced in their physicochemical properties by adding axial ligands. The porphyrin ligand serves as a platform for achieving desirable molecular and materials properties, such as very large dipole moments, polarizabilities, or hyperpolarizabilities [5, 6].

*Corresponding authors. Email: Tatyana.Shubina@chemie.uni-erlangen.de; Tim.Clark@chemie.uni-erlangen.de
†Dedicated to Professor Rudi van Eldik on the occasion of his 65th birthday.

Journal of Coordination Chemistry
ISSN 0095-8972 print/ISSN 1029-0389 online
DOI: 10.1080/00958972.2010.503346

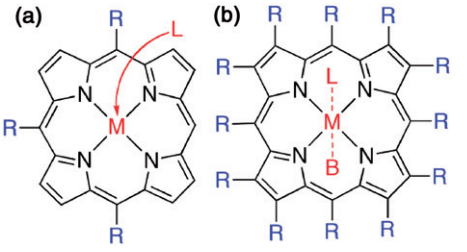

Scheme 1. Five- (a) and six-coordinate (b) complexes of MP. B can be any Lewis base.

Generally, fourfold and fivefold coordination models are used to describe MPs. In the fourfold coordination model, the metal is coordinated to the porphyrin nitrogens and the lower coordination site remains free (scheme 1a). The upper coordination site can later be occupied by ligands such as H_2O, CO, O_2, NO, etc.

This model represents a natural starting point for both experimental and theoretical studies. Crystal structures have been reported for a number of heme derivatives with different substituents in the ring [7]. FeTPP (TPP = *meso*-tetraphenylporphyrin) has been particularly widely used. Its electronic state is known experimentally to correspond to a low-spin triplet ($S = 1$).

Coordination of a base (e.g., the imidazole (Im) ligand) to the heme group leads to a five-coordinate species with square pyramidal geometry.

Coordination of small organic molecules by porphyrin complexes gives rise to either five- or six-coordinate ligand–MP complexes (equations (1) and (2)):

$$\mathrm{MP} + \mathrm{L} \rightleftharpoons \mathrm{MP{-}L} \tag{1}$$

$$\mathrm{MP(B)} + \mathrm{L} \rightleftharpoons \mathrm{MP(B) - L} \tag{2}$$

The data obtained in quantitative studies of these equilibria have been summarized in a review [8]. These equilibria can easily be shifted in the desired direction by changing the concentrations of ligands, the nature of the solvent, or the temperature. Coordination of additional ligands is accompanied by a shift of 5–35 nm of the absorption bands in the optical spectrum relative to those of the starting MP. The value and direction of the shift depend on the nature of the central atom and the ligand and on the structure of porphyrin. The addition of the ligand leads to a bathochromic shift of the first absorption band, which corresponds to a low-frequency $\pi \rightarrow \pi^*$ transition, if the MP is planar and binds solvent molecules weakly.

Because of the diversity of polyhedral geometries found in porphyrin complexes with metal cations, additional ligands exhibit many different coordination modes. In Fe^{II}, Co^{II}, Mn^{II}, Zn^{II}, etc. complexes with one extra ligand, MP–L, the metal ion is pushed out of the N_4 plane, and the MN_4 coordination unit can be described as a pyramid with the M metal in the apical position.

Consequently, there has been much interest in understanding the electronic structure of these molecules. Since the partial occupancy of the 3d shell can yield a number of low-lying electronic states within a narrow energy range, there has long been a debate as to what is the ground state for unligated, four-coordinate Fe(II) and Co(II) porphyrins (FeP and CoP, respectively).

There have been many studies that discuss the performance of various density functional theory (DFT) functionals for MPs. It is now generally accepted that the ground state of FeP is intermediate spin; only the $^3A_{2g}$ state arising from the $(d_{z^2})^2(d_{xy})^2(d_{\pi})^2$ configuration is compatible with Mössbauer, magnetic moment, and proton nuclear magnetic resonance (NMR) data [9–13]. The standard B3LYP functional suggests the ground state to be $^3A_{2g}$, in agreement with most of the experiments [14]. For low-spin ($S = 1/2$) CoP, the ground state configuration is known to be $^2A_{1g}$ $\{(d_{xy})^2(d_{xz})^2(d_{yz})^2(d_{x^2-y^2})^0(d_{z^2})^1\}$. However, the ^2E_g state is only 0.2 eV higher in energy than the $^2A_{1g}$ ground state.

Additionally, the axial ligands influence the electronic structure of metal porphyrins. It is known that axial ligation has a substantial influence on the redox [15, 16] and photovoltaic [17] properties of metal porphyrins. For example, iron porphyrins with coordinating axial ligands are diamagnetic ($S = 0$) in contrast to four-coordinate species ($S = 1$) [18, 19]. Elucidating the electronic structure of metal porphyrins with axial ligands is also important for understanding their biological and catalytic functions [20].

There are generally two reasons why accurate prediction of MP–L binding energies might be difficult, especially for DFT. First, the spin state of the metal ion may change during the ligand addition (i.e., FeP/FeP–NO or CoP/CoP–NO) [21], while the relative energies of different spin states for transition metal complexes require a high-level description of electronic exchange and correlation. Second, the energy of a covalent M–L bond contains an important contribution from non-dynamic correlation.

2. Methods

All DFT calculations were performed using local generalized gradient approximation (GGA) (BLYP [22–24], OLYP [23–26]), hybrid GGA (B3LYP [27–30], B3PW91 [31–34]), and meta-GGA (M06L [35]) functionals using the 6–31G(d) [36–46] and 6–311+G(d,p) basis sets. B3LYP in combination with the 6–31G(d,p) basis set with the LANL2DZ [47–49] basis set with pseudopotentials for Co and Fe (denoted as B3LYP/GEN) calculations were also performed. Stationary points were confirmed to be minima or transition states by calculating the normal vibrations within the harmonic approximation. All DFT-computed relative energies are corrected for zero-point vibrational energies (ZPE).

For comparison with the DFT results, all structures were fully optimized at the MP2 [50–55] level of theory using the 6–31G(d) and cc–pVDZ [56] basis sets. The Gaussian 09 program package [57] was used for all calculations. Additional single-point complete active space self-consistent field/complete active space with second-order perturbation theory (CASSCF/CASPT2) calculations were performed with the Molcas 7.4 package [58] using a Cholesky decomposition scheme [59] for the two-electron integrals. ANO-RCC-VTZ [60–62] basis sets were used in the CASSCF calculations.

We used different levels of theory because it is not clear [63, 64] which combination of density functional and basis set is appropriate for treating MP systems.

Three spin (low, intermediate, and high) states were considered for FeP, and only the low-spin state for CoP porphyrins and for the resulting complexes of FeP and CoP with CO and NO ligands.

Table 1. Spin multiplicities and relative energies ($\Delta E + \text{ZPE}$) of FeP.

	ΔE (kcal mol^{-1})		
FeP	$S = ½\ ^1A_{1g}$	$S = 3/2\ ^3A_{2g}$	$S = 5/2\ ^5A_{2g}$
BLYP/6–31G(d)	41.3	0.0	14.8
BLYP/6–311 + G(d,p)	33.0	0.0	14.6
B3LYP/6–31G(d)	41.5	0.0	4.3
B3LYP/6–311 + G(d,p)	34.2	0.0	4.3
B3LYP/GEN	31.7	0.0	4.0
B3PW91/6–31G(d)	41.4	0.0	2.5
B3PW916–311 + G(d,p)	34.2	0.0	2.5
OLYP/6–31G(d)	39.9	0.0	3.1
OLYP/6–311 + G(d,p)	Does not converge	0.0	3.1
M06L/6–31G(d)	30.6	0.0	−2.4
M06L/6–311 + G(d,p)	26.6	0.0	−2.8
MP2/6–31G(d)	43.4	0.0	–
MP2/cc–pVDZ	35.4	0.0	–

3. Results and discussion

3.1. *Fe(II)P and Co(II)P*

In the case of FeP, it is generally agreed [65] that pure DFT methods usually overestimate the stability of the low-spin states and hybrid functionals predict smaller quintet–triplet gaps, often resulting in the quintet ground state. Both low-lying triplet and quintet states have been reported to be the ground state. No experimental data have yet been reported for gas-phase FeP or CoP molecules. Hence, the calculated properties of the parent MPs are usually compared to substituted Fe(II) or Co(II) porphyrins, tetraphenyl (TPP), octaethyl tetraphenyl (OETPP), and others. Several experimental studies [9, 10, 13] have demonstrated that FeTPP is a triplet and CoTPP is a doublet. Thus, we only consider the $^1A_{1g}$, $^3A_{2g}$, and $^5A_{2g}$ (in case of FeP) and $^2A_{1g}$ (in case of CoP) states here, rather than all possible low-lying spin states. As shown in table 1, the lowest energy spin state is a triplet in all cases except with M06L, and the relative spin-state energy order predicted is $(S = 3/2) < (S = 5/2) < (S = 1/2)$. The M06L method favors the quintet state over the triplet by up to 2.8 kcal mol^{-1} (table 1). Changing from the 6−31G(d) to the 6−311+G(d,p) basis set only affects singlet–triplet gap, decreasing it by 5–7 kcal mol^{-1} (table 1). The calculated triplet–quintet gap depends less on the basis set, with the calculated energies varying by −0.4 to +0.2 kcal mol^{-1}. The calculated triplet–quintet gap for the FeP–Im system has been reported to vary from −0.8 to 2.6 kcal mol^{-1} [65].

In all cases, the computed $\langle S^2 \rangle$ values are very close to the pure states (2.02 *vs.* 2.0 for triplet and 6.02 *vs.* 6.0 for quintet). This is also true for CoP ($\langle S^2 \rangle$ is 0.75–0.76 *vs.* 0.75 for the doublet state).

3.2. *FeP and CoP complexes with carbon monoxide*

Tables 2 and 3 present the results of DFT and MP2 calculations for the Fe–CO and Co–CO systems. The displacement of both metals with respect to the N plane is up

Table 2. Number of imaginary frequencies (N_i), binding energy ($\Delta E + ZPE$), and the key structural parameters (Co–CO and C–O bond lengths and M–C–O angle) of CoP–CO unit.

Method	N_i	E_{bind} (kcal mol^{-1})	Co–C (Å)	C–O (Å)	∠Co–C–O (°)
BLYP/6–31G(d) C_{4v}	2	−19.6	1.852	1.164	180.0
BLYP/6–31G(d)	0	−19.6	1.862	1.166	158.1
BLYP/6–311 + G(d,p) C_{4v}	0	−10.1	1.907	1.153	180.0
BLYP/6–311 + G(d,p)	0	−10.1	1.905	1.153	179.9
B3LYP/6–31G(d) C_{4v}	2	−9.1	1.949	1.142	180.0
B3LYP/6–31G(d)	0	−9.2	1.959	1.143	158.4
B3LYP/GEN C_{4v}	2	−4.2	2.231	1.136	180.0
B3LYP/GEN	0	−4.2	2.245	1.136	167.4
B3LYP/6–311 + G(d,p) C_{4v}	0	−2.7	2.054	1.131	180.0
B3PW91/6–31G(d) C_{4v}	2	−9.9	1.921	1.141	180.0
B3PW91/6–31G(d)	0	−9.8	1.917	1.141	180.0
B3PW91/6–311 + G(d,p) C_{4v}	0	−4.5	1.999	1.131	180.0
B3PW91/6–311 + G(d,p)	0	−4.5	2.001	1.131	179.9
OLYP/6–31G(d) C_{4v}	2	−14.3	1.838	1.161	180.0
OLYP/6–31G(d)	0	−14.3	1.844	1.163	159.6
OLYP/6–311 + G(d,p) C_{4v}	0	−6.4	1.883	1.152	180.0
M06L/6–31G(d) C_{4v}	2	−18.1	1.894	1.150	180.0
M06L/6–31G(d)	0	−18.0	1.904	1.153	152.9
M06L/6–311 + G(d,p) C_{4v}	0	−11.3	1.968	1.140	180.0
M06L/6–311 + G(d,p)	0	−11.3	1.975	1.141	161.7
MP2/6–31G(d) C_{4v}	3	−11.6	2.193	1.148	180.0
MP2/6–31G(d)	0	−12.4	2.200	1.150	149.1
MP2/cc–pVDZ C_{4v}	0	–	2.308	1.145	180.0

Table 3. Number of imaginary frequencies (N_i), binding energy ($\Delta E + ZPE$), and the key structural parameters (Fe–CO and C–O bond lengths and Fe–C–O angle) of FeP–CO unit.

Method	N_i	E_{bind} (kcal mol^{-1})	Fe–C (Å)	C–O (Å)	∠Fe–C–O (°)
BLYP/6–31G(d) C_{4v}	0	−26.6	1.699	1.176	180.0
BLYP/6–311 + G(d,p) C_{4v}	0	−22.7	1.723	1.167	180.0
B3LYP/6–31G(d) C_{4v}	0	−6.8	1.717	1.154	180.0
B3LYP/6–311 + G(d,p) C_{4v}	0	−4.4	1.746	1.144	180.0
B3LYP/GEN C_{4v}	0	−6.7	1.736	1.151	180.0
B3PW91/6–31G(d) C_{4v}	0	−9.6	1.699	1.154	180.0
B3PW91/6–311 + G(d,p) C_{4v}	0	−8.4	1.724	1.144	180.0
OLYP/6–31G(d) C_{4v}	0	−23.8	1.676	1.173	180.0
OLYP/6–311 + G(d,p) C_{4v}	0	−20.3	1.694	1.165	180.0
M06L/6–31G(d) C_{4v}	0	−29.1/(−26.7)[a]	1.697	1.162	180.0
M06L/6–311 + G(d,p) C_{4v}	0	−25.1/(−22.3)[a]	1.719	1.154	180.0
MP2/6–31G(d) C_{4v}	0	1.6	1.645	1.168	180.0
MP2/cc–pVDZ C_{4v}	0	4.0	1.748	1.155	180.0
Exp [73]			1.77(2)	1.12(2)	179(2)
Fe(OEP)CO [74]			1.7140	1.1463	177.2

[a]With respect to ^{5}FeP.

to 0.1 Å. CO binding to Fe in FeP leads to a linear orientation of the M–C–O unit (C_{4v}, figure 1). In a protein matrix, the geometry of the Fe–C–O unit is somewhat distorted, but this is mainly because of the electrostatic perturbation from the distal environment [66–68]. An equivalent linear structure of CoP–CO was found to be a second-order saddle point ($N_i = 2$) when the 6−31G(d) basis set was used.

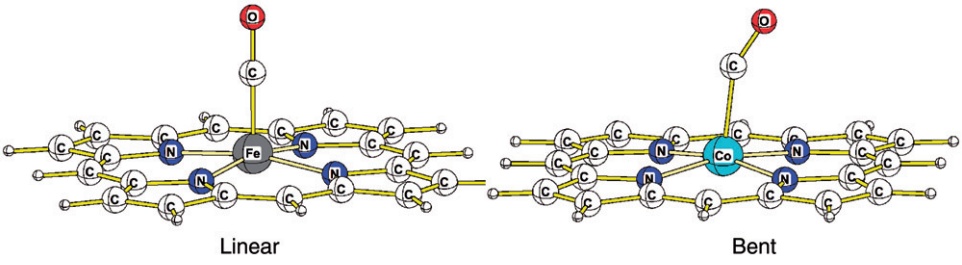

Figure 1. Linear and bent arrangements of CO unit in MP–CO complexes.

Re-optimization of this complex without symmetry restrictions leads to the energetically almost equivalent complex with a bent Co–CO moiety (figure 1 and table 2). Optimization of C_{4v}-linear complexes with the 6−311+G(d,p) basis set gives minima and optimization of bent starting geometries results in linear structures. The same preference for a bent CoP–CO structure is found with MP2.

The reaction of cobalt(II) porphyrins with CO has been studied by Wayland *et al.* [69–72] in some detail by electron paramagnetic resonance (EPR) in frozen solutions. They conclude that Co(II)TPP forms an axially symmetric weakly bonded 1 : 1 adduct with CO [69–72]. To the best of our knowledge, there are no other studies on CoP–CO complexes, neither experimental, nor theoretical.

Table 2 presents that the calculated CO binding energy, Co–CO and C–O bond lengths vary significantly. CoP–CO bond lengths vary from 1.838 (OLYP) to 1.949 Å (B3LYP) using the 6−31G(d) basis set. An even longer Co–CO bond length was found at the B3LYP/GEN and MP2/6−31G(d) levels (up to 2.245 Å, table 2). Using a larger basis set {6−311+G(d,p)} leads to a lengthening of the M−CO bond (by 0.05 Å, relative to the 6–31G(d) results) and to shortening of the C–O bond (table 2). The CO binding energy to CoP varies from −9.2 (B3LYP) to −19.6 kcal mol^{-1} (BLYP) with the 6–31G(d) basis set, and from −2.7 (B3LYP) to −11.3 (M06L) with the 6–311+G(d,p) basis set. The MP2 calculated binding energy was found to be −12.4 kcal mol^{-1}.

The results are similar for the FeP–CO system. The Fe–CO bond length varies with the method used (from 1.676, OLYP/6−31G(d) to 1.746 Å, B3LYP/6−311+G(d,p), table 3). The experimental value is 1.77(2) Å for the six-coordinate FeTPP(Py)–CO complex [73]. A much shorter bond length of 1.7140 Å (Fe–C) was reported for five-coordinate Fe(OEP)CO [74]. CO binding energies were calculated to be in the range of −4.4 kcal mol^{-1} (B3LYP/6−311+G(d,p) to −26.6 (BLYP) kcal mol^{-1} (table 3). In a Car–Parrinello molecular dynamics study, the Fe−CO distance was found to be 1.69 Å and a CO binding energy of 26 kcal mol^{-1} was reported [75–77]. In other DFT studies, the reported binding energies are between +1.0 and −26.5 kcal mol^{-1} [78]. Calculated binding energies for the six-coordinate FeP(Im)–CO system lie between +1.0 and −40.6 kcal mol^{-1} (B3LYP) [78]. Gromacs MD simulations of CO binding to solvated myoglobin gave an activation enthalpy of −7 to −11 kcal mol^{-1} [79, 80]. Experimental values of −18.1 and −19.5 kcal mol^{-1} have also been reported for a six-coordinate complex [81, 82].

Thus, the data given in table 3 suggest that combination of the B3PW91 functional with the 6−311+G(d,p) basis is best suited for describing the FeP−CO complex. We also note that while the MP2/cc-pVDZ computed geometry is close to those

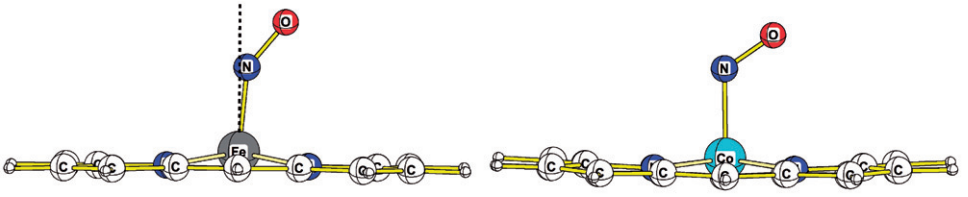

Figure 2. FeP–NO (left) and CoP–NO (right) complexes.

Table 4. Binding energy ($\Delta E + ZPE$) and key structural parameters (Fe–NO and N–O bond lengths and Fe–N–O angle) of Fe–NO system.

	E_{bind} (kcal mol^{-1})	Fe–NO (Å)	N–O (Å)	∠Fe–N–O (°)
BLYP/6–31G(d)	−39.8	1.703	1.198	143.2
BLYP/6–311 + G(d,p)	−35.1	1.719	1.187	144.6
B3LYP/GEN	−6.5	1.731	1.169	139.9
B3LYP/6–31G(d)	−14.4	1.796	1.182	139.6
B3LYP/6–311 + G(d,p)	−10.6	1.809	1.169	142.2
B3PW91/6–31G(d)		Does not converge		
B3PW91/6–311 + G(d,p)	−13.7	1.782	1.164	144.4
OLYP/6–31G(d)	−36.3	1.688	1.185	144.8
OLYP/6–311 + G(d,p)	−32.0	1.701	1.175	146.2
M06L/6–31G(d)	−41.4/(−39.0)[a]	1.707	1.181	140.6
M06L/6–311 + G(d,p)	−37.4/(−34.6)[a]	1.726	1.169	141.6
MP2/6–31G(d)		Does not converge		
MP2/cc–pVDZ	7.59	2.249	1.135	124.5
Tape-FeTPP [85, 86]	−39.6			148
Exp [81, 82, 87]	−26.6, −28.9, −22.8			
Exp [84]		1.71(1)	1.12(1)	149(1)

[a]With respect to ^{5}FeP.

obtained with DFT functionals, the CO binding energy was found to be +4 kcal mol^{-1} (table 3).

3.3. *FeP and CoP complexes with nitric oxide*

Because of the importance of the nitrosyl–heme (Fe(II)P) complex [14, 64, 78], a number of theoretical studies have been reported, but only a few [78, 83] on nitrosyl–Co(II)P. In the case of FeP, NO is attached in the so-called "end-on" configuration, and the complex has C_s symmetry. The Fe is displaced (between 0.2 and 0.3 Å) with respect to the N_4 plane, and the Fe−N bond is displaced 6–8° from what would be the C_4 symmetry axis in the linear structure (figure 2). The Fe–NO bond length lies between 1.69 (OLYP) and 1.81 Å (B3LYP/6−311+G(d,p)); the Fe−N−O angle between 139.6° and 146.2° (table 4).

The experimental values [84] based on X-ray data for FeTPP–NO are 1.71(1) Å and 149(1) Å, respectively. These values are reproduced well by BLYP/6−311+G(d,p) OLYP/6−311+G(d,p), and M06L/6−31G(d). On the other hand, MP2 gives a very

Table 5. Binding energy ($\Delta E + ZPE$) and key structural parameters (Co–NO and N–O bond lengths and Co–N–O angle) of the Co–NO system.

	E_{bind} (kcal mol^{-1})	Co–NO (Å)	N–O (Å)	∠Co–N–O (°)
BLYP/6–31G(d)	−36.7	1.795	1.195	123.2
BLYP/6–311 + G(d,p)	−28.3	1.834	1.182	122.7
B3LYP/GEN	−2.2	1.839	1.169	118.7
B3LYP/6–31G(d)	−11.5	1.790	1.175	120.5
B3LYP/6–311 + G(d,p)	−3.6	1.828	1.161	120.2
B3PW91/6–31G(d)	−12.9	1.773	1.171	120.7
B3PW91/6–311 + G(d,p)	−5.1	1.809	1.157	120.3
OLYP/6–31G(d)	−30.3	1.780	1.183	123.8
OLYP/6–311 + G(d,p)	−23.6	1.814	1.172	123.3
M06L/6–31G(d)	−30.8	1.786	1.181	120.7
M06L/6–311 + G(d,p)	−25.5	1.822	1.167	120.4
MP2/6–31G(d)	−13.8	1.878	1.137	116.2
MP2/cc–pVDZ		Does not converge		
Tape-CoTPP-NO [85, 86]	−39.6			123
Exp [89]	*ca* −21 to −25			
Co(OEP)–NO [88]		1.8444	1.1642	122.7
CoT(*p*-OCH$_3$)PP–NO		1.855(6)	1.159(8)	120.6

long Fe–NO bond length (2.25 Å) and predicts a Fe–N–O angle of only 124.5°. Based on this and the computed NO binding energy, the FeP–NO complex can be described as being unbound at the MP2 level. Binding energies obtained with DFT range from −6.5 kcal mol^{-1} (B3LYP/GEN) to −41.4 (M06L). Values reported in previous theoretical studies range from −0.9 to −38 kcal mol^{-1} for five-coordinate complexes [77, 78] and from +5.3 to −43 kcal mol^{-1} for six-coordinate complexes [78]. Experimental binding energies are −26.6 and −28.9 kcal mol^{-1} for five-coordinate complexes [81, 82], −39.6 kcal mol^{-1} (tape-FeTPP–NO) [85, 86], and −22.8 kcal mol^{-1} (for a six-coordinate complex) [87].

In contrast to FeP–NO, the direction of the Co–N in CoP–NO is nearly perpendicular to the porphyrin plane (we found a tilt of the Co–N bond of only 0.4°) and the Co is displaced from the N_4 plane by only 0.1–0.2 Å. These findings are in a good agreement with X-ray data on Co(OEP)–NO [88] and CoT(*p*-OCH$_3$)PP–NO (table 5).

Once again, the geometries and NO binding energy depend strongly on the method used. The Co–NO bond length was found to lie between 1.77 (B3PW91) and 1.88 Å (MP2/6–31G(d)) and the Co–N–O angle between 116.2° and 123.8° (table 5). Zhu *et al.* [89] estimated the homolytic Co^{II}–NO bond dissociation energy to be 20.8–24.6 kcal mol^{-1} in benzonitrile solution. Our computed NO binding energy ranges from −2.2 (B3LYP/GEN) to −36.7 kcal mol^{-1} (BLYP) (table 5). Both the OLYP/6–311+G(d,p) and M06L/6–311+G(d,p) methods agree well with the experimental values. In the case of CoP–NO, MP2/6–31G(d) performs reasonably well in describing geometry and binding energy compared to various DFT functionals (table 5). However, it still underestimates the binding energy.

3.4. *CASSCF/CASPT2 calculations*

We performed CASSCF/CASPT2 calculation based on B3LYP/6–31G(d) optimized geometries of CoP–CO (C_1), FeP–CO (C_{2v}), and Co/Fe–NO (C_s) complexes in order to

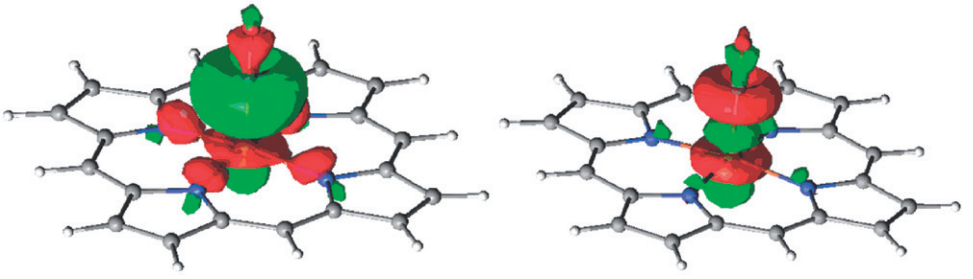

Figure 3. Bonding (left) and antibonding (right) orbitals for the FeP–CO σ bond.

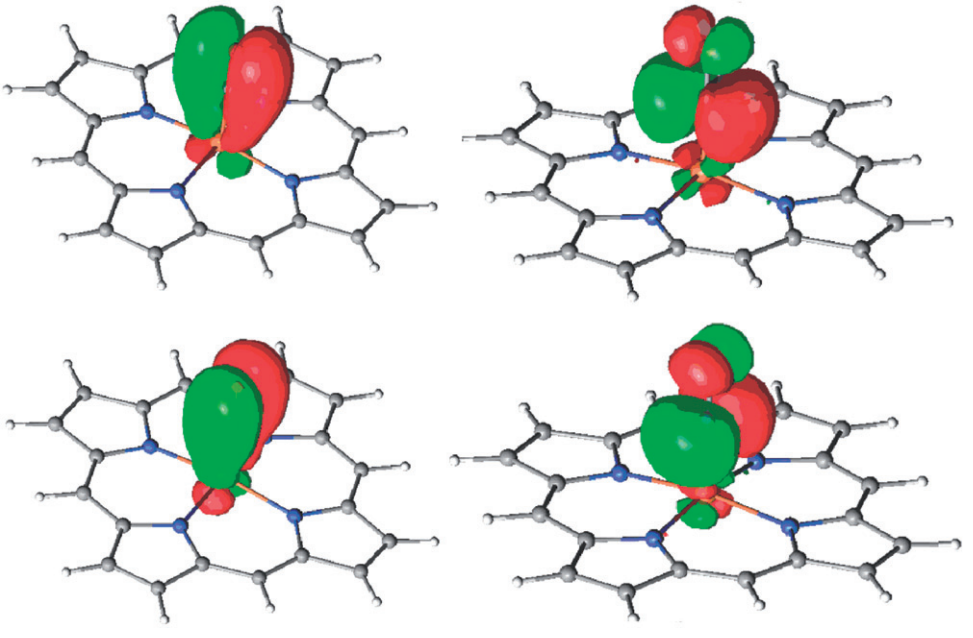

Figure 4. Bonding (left) and antibonding (right) orbitals for the FeP–CO π bond.

analyse the nature of the interactions of CoP/FeP with CO and NO. The active space in the CASSCF method comprised five 3d orbitals of the metal, four correlating 3d′ orbitals to singly and doubly occupied 3d orbitals [90, 91], and a combination of nitrogen-free electron pair orbital correlation to the unoccupied $3d_{x^2-y^2}$ orbital, plus the corresponding p orbitals of CO and NO. This gives an active space of 14 orbitals and 15 electrons (denoted as 15,14) for CoP–CO, (14,14) for FeP–CO/CoP–NO and (13,14) for FeP–NO. Adding the second d orbital shell (3d′) is necessary to account for the strong radial correlation effects in the localized 3d orbitals.

For the coordination of CO to FeP and CoP, the interaction can be rationalized in terms of a "traditional" σ-donation/π-back-donation mechanism. The FeP–CO σ bond is formed by the $3d_{z^2}$ orbital on iron (occupation number of 0.38e) and the $2p_z$ orbital on CO (0.55e, Cp_z) (figure 3). The π bonds are formed by back-donation from the FeP d_π and p_π orbitals to the π*-antibonding orbitals of CO (figure 4). The major

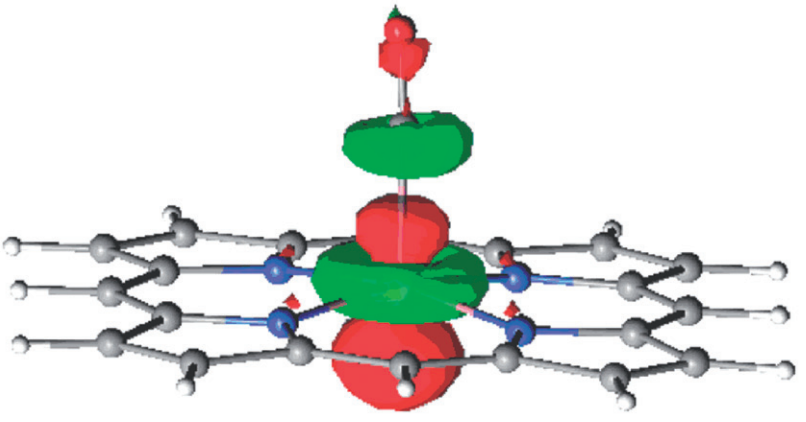

Figure 5. Singly occupied molecular orbital (SOMO) for the CoP–CO σ bond.

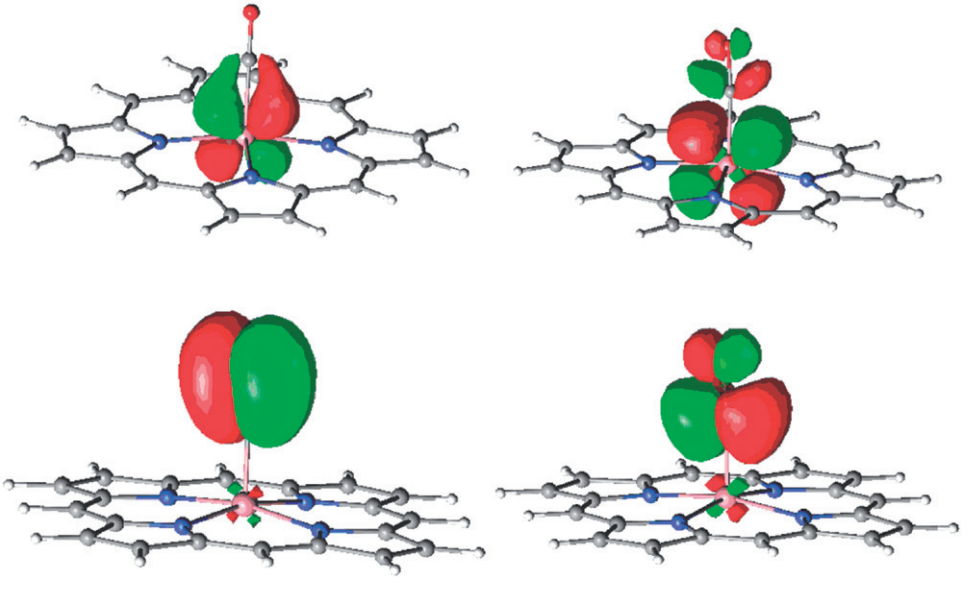

Figure 6. Bonding (left) and antibonding (right) orbitals of CoP–CO π bond.

contributions arise from combination of $3d_{xz}$ (0.35e) with the $2p_x$ orbitals of the carbon (0.45e) and oxygen (0.65e) and $3d_{yz}$ (0.35e) with the $2p_y$ orbitals of the carbon (0.45e) and oxygen (0.65e). The Mulliken charges are +0.47e for Fe and +0.17e for the CO moiety.

Compared to FeP–CO $\{d^6\text{–}CO\pi^{*0}\}$, the CoP–CO complex has an additional single unpaired electron $\{d^7\text{–}CO\pi^{*0}\}$ in the $3d_{z^2}$ orbital (0.5e), which is used in σ bonding with CO (C 2s, $0.44e + 2p_z$, 0.21e) (figure 5).

The π-back-donation from the CoP d_π orbitals is much less pronounced than for FeP (figure 6) and is mainly determined by a combination of four orbitals: $3d_{xz}$ (−0.98e) + C

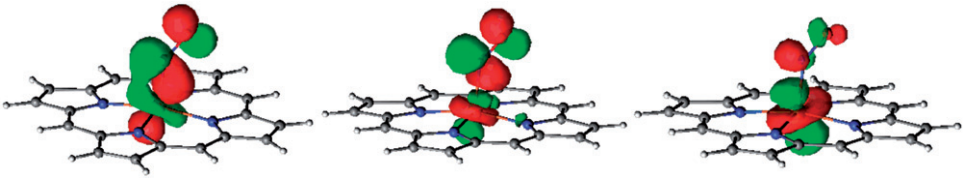

Figure 7. Bonding (left), antibonding (middle), and SOMO (right) orbitals in the FeP–NO complex.

Figure 8. Bonding (left) and antibonding (right) orbitals in the CoP–NO complex.

$2p_x$ (0.1e); $3d_{yz}$ (0.98e) + C $2p_y$ (−0.1e); $3d_{xz}$ (−0.1e) + C $2p_x$ (−0.4e) + O $2p_x$ (−0.8e); and $3d_{yz}$ (0.1e) + C $2p_y$ (0.4e) + O $2p_y$ (0.8e) (figure 6). The charge on Co was found to be 0.68e and the total charge for the CO moiety −0.17e. Previously [71, 72], CO was estimated to carry 0.13e. It should also be noted that there is a much higher contribution of the d orbitals from the second d shell. The difference between doublet and quartet states of CoP–CO was found to be 19.6 kcal mol^{-1} at BLYP/6–31G(d) and only 2.2 kcal mol^{-1} at CASSCF.

The bonding of NO to both FeP and CoP occurs in a bent fashion, and there is much more pronounced electron transfer from metal to the ligand (0.74e) in comparison to CO. In the case of FeP–NO $\{d^6$–NO$\pi^{*1}\}$ there is a single unpaired electron on the $3d_{z^2}$ orbital (FeP–NO is isoelectronic to CoP–CO) and the CoP–NO complex has a singlet ground state $\{d^7$–NO$\pi^{*1}\}$.

The bonding orbital in FeP–NO (figure 7) consists of the combination of $3d_{z^2}$ (−0.68e) + $2p_x$ and $2p_y$ orbitals of the nitrogen and oxygen.

A similar picture is found for CoP and NO (figure 8): the bonding can be described as a σ bond between the $3d_{z^2}$ of Co and the π^* orbital of NO ($2p_{xN+O}$ and $2p_{yN+O}$). The smaller Co–N–O angle (120–123°) than that found for Fe–N–O (140–145°) facilitates overlap between these two orbitals.

The CASSCF computed spin densities for the doublet states of FeP–NO and CoP–CO show that the unpaired electron is localized predominantly on the metal, while NO and CO carry negligible spin density (Fe: 1.06e, NO: −0.08e, Co: 0.9e, and CO: −0.07e). Thus, both complexes can be described as M(I)P–XO^+.

4. Conclusions

The CO and NO complexes with cobalt(II) and iron(II) porphyrins have been investigated theoretically with five DFT functionals (BLYP, B3LYP, OLYP, B3PW91,

and M06L), MP2, and CASSCF/CASPT2 approaches. None of the optimized structures show significant spin contamination. The M06L functional favors quintet state of FeP over the triplet by 2.8 kcal mol^{-1}, all other functionals tested predict the triplet to be the lowest state.

The computed binding energies of CO and NO to Co(II)P and Fe(II)P depend strongly on the method and the basis set used. The combination of B3LYP with 6−31G(d,p) and LANL2DZ basis sets turns out to be the worst of the DFT levels tested for describing CO and NO complexes of MPs [92]. MP2 fails completely to describe the geometries and binding energies of the FeP–CO, CoP–CO, and CoP–NO complexes, but performs much better for FeP–NO.

In the complete absence of experimental data on the geometries of CoP–CO, it is difficult to validate the results obtained with different DFT functionals. However, the EPR spectra suggest linearity of Co–C–O unit, so that this system should be described at least with a triple-ξ quality basis set. For FeP–CO and FeP–NO/CoP–NO, B3PW91/6−311 + G(d,p) and OLYP/6−311 + G(d,p) are the best choices, respectively, of the methods tested.

Acknowledgments

The authors thank Prof. Laura Gagliardi (University of Minnesota) and Dr Tanya Todorova (University of Geneva) for providing valuable discussions. This study was supported by the Deutsche Forschungsgemeinschaft as part of SFB583 "Redox-Active Metal Complexes: Control of Reactivity *via* Molecular Architecture" and by a grant of computer time on the Höchstleistungsrechner in Bayern II (HLRB II).

References

[1] S.K. Chapman, S. Daff, A.W. Munro. *Struct. Bond.*, **88**, 39 (1997).
[2] D.M. Greenwoord (Ed.). *Metabolic Pathways*, Academic Press, New York (1969).
[3] D.F.V. Lewis. *Cytochromes P450: Structure, Function and Mechanism*, Taylor and Francis, London (1996).
[4] S.I. Beale. *Photosynth. Res.*, **24**, 95 (2002).
[5] K.S. Suslick, N.A. Rakow, M.E. Kosal, J.-H. Chou. *J. Porphyrins Phthalocyanines*, **4**, 407 (2000).
[6] K.S. Suslick, C.T. Chen, G.R. Meredith, L.T. Cheng. *J. Am. Chem. Soc.*, **114**, 6928 (1992).
[7] W.R. Scheidt, M.K. Ellison. *Acc. Chem. Res.*, **32**, 350 (1999).
[8] B.D. Berezin, O.I. Koifman. *Usp. Khimii, Russ. Chem. Rev.*, **49**, 2389 (1980).
[9] J.P. Collman, J.L. Hoard, N. Kim, G. Lang, C.A. Reed. *J. Am. Chem. Soc.*, **97**, 2676 (1975).
[10] G. Lang, K. Spartalian, C.A. Reed, J.P. Collman. *J. Chem. Phys.*, **69**, 5424 (1978).
[11] P.D.W. Boyd, A.D. Buckingham, R.F. McMecking, S. Mitra. *Inorg. Chem.*, **18**, 3585 (1979).
[12] H. Goff, G.N. La Mar, C.A. Reed. *J. Am. Chem. Soc.*, **99**, 3641 (1977).
[13] J. Mispelter, M. Momenteau, J.M. Lhoste. *J. Chem. Phys.*, **72**, 1003 (1980).
[14] P.M. Kozlowski, T.G. Spiro, A. Berces, Z. Zgierski. *J. Phys. Chem. B*, **102**, 2603 (1998).
[15] P. Cocolios, K.M. Kadish. *Isr. J. Chem.*, **25**, 138 (1985).
[16] K. Takahashi, T. Komura, H. Imanaga. *Bull. Chem. Soc. Jpn.*, **62**, 386 (1989).
[17] C.H. Langford, S. Seto, B.R. Hollebone. *Inorg. Chim. Acta*, **90**, 221 (1984).
[18] H. Kobayashi, Y. Yanagawa. *Bull. Chem. Soc. Jpn.*, **45**, 450 (1972).
[19] S.M. Peng, J.A. Ibers. *J. Am. Chem. Soc.*, **98**, 8032 (1976).
[20] J.L. Que, W.B. Tolman. *Nature*, **455**, 333 (2008).
[21] G.G. Gibson, P.P. Tamburini. *Xenobiotica*, **14**, 27 (1984).
[22] A.D. Becke. *Phys. Rev. A*, **38**, 3098 (1988).

[23] C. Lee, W. Yang, R.G. Parr. *Phys. Rev. B*, **37**, 785 (1988).
[24] B. Miehlich, A. Savin, H. Stoll, H. Preuss. *Chem. Phys. Lett*., **157**, 200 (1989).
[25] N.C. Handy, A.J. Cohen. *Mol. Phys*., **99**, 403 (2001).
[26] W.-M. Hoe, A.J. Cohen, N.C. Handy. *Chem. Phys. Lett*., **341**, 319 (2001).
[27] A.D. Becke. In *The Challenge of d- and f-Electrons: Theory and Computation*, D.R. Salahub, M.C. Zerner (Eds), p. 165, American Chemical Society, Washington DC (1989).
[28] S.H. Vosko, L. Wilk, M. Nusair. *Can. J. Phys*., **58**, 1200 (1980).
[29] C. Lee, W. Yang, R.G. Parr. *Phys. Rev. B*, **37**, 785 (1988).
[30] A.D. Becke. *J. Chem. Phys*., **98**, 5648 (1993).
[31] J.P. Perdew. In *Electronic Structure of Solids*, P. Ziesche, H. Eschrig (Eds), pp. 11–20, Akademie Verlag, Berlin (1991).
[32] B. König, S. Ramm, P. Bubenitschek, P.G. Jones, H. Hopf, B. Knieriem, A. de Meijere. *Chem. Ber*., **127**, 2263 (1994).
[33] J.P. Perdew, K. Burke, Y. Wang. *Phys. Rev. B*, **54**, 16533 (1996).
[34] J.P. Perdew, J.A. Chevary, S.H. Vosko, K.A. Jackson, M.R. Pederson, D.J. Singh, C. Fiolhais. *Phys. Rev. B*, **46**, 6671 (1992).
[35] Y. Zhao, D.G. Truhlar. *Theor. Chem. Acc*., **120**, 215 (2008).
[36] R.C.J. Binning, L.A. Curtiss. *J. Comp. Chem*., **11**, 1206 (1990).
[37] J.-P. Blaudeau, M.P. McGrath, L.A. Curtiss, L. Radom. *J. Chem. Phys*., **107**, 5016 (1997).
[38] R. Ditchfield, W.J. Hehre, J.A. Pople. *J. Chem. Phys*., **54**, 724 (1971).
[39] M.M. Francl, W.J. Pietro, W.J. Hehre, J.S. Binkley, D.J. DeFrees, J.A. Pople, M.S. Gordon. *J. Chem. Phys*., **77**, 3654 (1982).
[40] M.J. Frisch, J.A. Pople, J.S. Binkley. *J. Chem. Phys*., **80**, 3265 (1984).
[41] M.S. Gordon. *Chem. Phys. Lett*., **76**, 163 (1980).
[42] P.C. Hariharan, J.A. Pople. *Theor. Chim. Acta*, **28**, 213 (1973).
[43] P.C. Hariharan, J.A. Pople. *Mol. Phys*., **27**, 209 (1974).
[44] W.J. Hehre, R. Ditchfield, J.A. Pople. *J. Chem. Phys*., **56**, 2257 (1972).
[45] V.A. Rassolov, J.A. Pople, M.A. Ratner, T.L. Windus. *J. Chem. Phys*., **109**, 1223 (1988).
[46] V.A. Rassolov, M.A. Ratner, J.A. Pople, P.C. Redfern, L.A. Curtiss. *J. Comp. Chem*., **22**, 976 (2001).
[47] T.H. Dunning Jr, P.J. Hay. *Modern Theoretical Chemistry*, Plenum, New York (1976).
[48] P.J. Hay, W.R. Wadt. *J. Chem. Phys*., **82**, 270 (1985).
[49] P.J. Hay, W.R. Wadt. *J. Chem. Phys*., **82**, 299 (1985).
[50] C. Møller, M.S. Plesset. *Phys. Rev*., **98**, 5648 (1934).
[51] M.J. Frisch, M. Head-Gordon, J.A. Pople. *Chem. Phys. Lett*., **166**, 275 (1990).
[52] M.J. Frisch, M. Head-Gordon, J.A. Pople. *Chem. Phys. Lett*., **166**, 281 (1990).
[53] M. Head-Gordon, T. Head-Gordon. *Chem. Phys. Lett*., **220**, 122 (1994).
[54] C. Moller, M.S. Plesset. *Phys. Rev*., **46**, 618 (1934).
[55] S. Saebo, J. Almlof. *Chem. Phys. Lett*., **154**, 83 (1989).
[56] T.H. Dunning Jr. *J. Chem. Phys*., **90**, 1007 (1989).
[57] M.J. Frisch, G.W. Trucks, H.B. Schlegel, G.E. Scuseria, M.A. Robb, J.R. Cheeseman, G. Scalmani, V. Barone, B. Mennucci, G.A. Petersson, H. Nakatsuji, M. Caricato, X. Li, H.P. Hratchian, A.F. Izmaylov, J. Bloino, G. Zheng, J.L. Sonnenberg, M. Hada, M. Ehara, K. Toyota, R. Fukuda, J. Hasegawa, M. Ishida, T. Nakajima, Y. Honda, O. Kitao, H. Nakai, T. Vreven, J.A. Montgomery, Jr, J.E. Peralta, F. Ogliaro, M. Bearpark, J.J. Heyd, E. Brothers, K.N. Kudin, V.N. Staroverov, R. Kobayashi, J. Normand, K. Raghavachari, A. Rendell, J.C. Burant, S.S. Iyengar, J. Tomasi, M. Cossi, N. Rega, N.J. Millam, M. Klene, J.E. Knox, J.B. Cross, V. Bakken, C. Adamo, J. Jaramillo, R. Gomperts, R.E. Stratmann, O. Yazyev, A.J. Austin, R. Cammi, C. Pomelli, J.W. Ochterski, R.L. Martin, K. Morokuma, V.G. Zakrzewski, G.A. Voth, P. Salvador, J.J. Dannenberg, S. Dapprich, A.D. Daniels, O. Farkas, J.B. Foresman, J.V. Ortiz, J. Cioslowski, D.J. Fox. *Gaussian 09*, Revision A.2, Gaussian, Inc., Wallingford, CT (2009).
[58] R.L.G. Karlström, P.-Å. Malmqvist, B.O. Roos, U. Ryde, V. Veryazov, P.-O. Widmark, M. Cossi, B. Schimmelpfennig, P. Neograd y, L. Seijo. *Comput. Mater. Sci*., **28**, 222 (2003).
[59] F. Aquilante, T.B. Pedersen, B.O. Roos, A. Sanchez de Meras, H. Koch. *J. Chem. Phys*., **129**, 024113 (2008).
[60] B.O. Roos, V. Veryazov, P.-O. Widmark. *Theor. Chim. Acta*, **111**, 345 (2004).
[61] B.O. Roos, R. Lindh, P.-A. Malmqvist, V. Veryazov, P.-O. Widmark. *J. Phys. Chem. A*, **108**, 2851 (2004).
[62] B.O. Roos, R. Lindh, P.-A. Malmqvist, V. Veryazov, P.-O. Widmark. *J. Phys. Chem. A*, **109**, 6575 (2005).
[63] M.-S. Liao, J.D. Watts, M.-J. Huang. *J. Comp. Chem*., **27**, 1577 (2006).
[64] M.-S. Liao, J.D. Watts, M.-H. Huang. *J. Phys. Chem. A*, **109**, 7988 (2005).
[65] D. Khvostichenko, A. Choi, R. Boulatov. *J. Phys. Chem. A*, **112**, 3700 (2008).
[66] T.G. Spiro, P.M. Kozlowski. *Acc. Chem. Res*., **34**, 137 (2001).
[67] K.M. Vogel, P.M. Kozlowski, M.Z. Zgierski, T.G. Spiro. *J. Am. Chem. Soc*., **43**, 9915 (1999).

[68] T.D. Lash. *J. Porphyrin Phthalocyanines*, **5**, 313 (2001).
[69] W. Cui, S. Li, B.B. Wayland. *J. Organomet. Chem.*, **692**, 3198 (2007).
[70] B.B. Wayland, A.E. Sherry, A.G. Bunn. *J. Am. Chem. Soc.*, **115**, 7675 (1993).
[71] B.B. Wayland, J.V. Minkiewicz, M.E. Abd-Elmageed. *J. Am. Chem. Soc.*, **96**, 2795 (1974).
[72] B.B. Wayland, D. Mohajer. *J. Am. Chem. Soc.*, **93**, 5296 (1971).
[73] S.-M. Peng, J.A. Ibers. *J. Am. Chem. Soc.*, **25**, 8032 (1976).
[74] N.J. Silvernail, B.C. Noll, C.E. Schulz, W.R. Scheidt. *Inorg. Chem.*, **45**, 7050 (2006).
[75] C. Rovira, P. Ballone, M. Parinello. *Chem. Phys. Lett.*, **271**, 247 (1997).
[76] C. Rovira, M. Parinello. *Chem. Eur. J.*, **5**, 250 (1999).
[77] C. Rovira, K. Kunc, J. Hutter, P. Ballone, M. Parinello. *J. Phys. Chem. A*, **101**, 8914 (1997).
[78] M. Radon, K. Pierloot. *J. Phys. Chem. A*, **112**, 11824 (2008).
[79] M. D'Abramo, A. Di Nola, A. Amadei. *J. Phys. Chem. B*, **113**, 16346 (2009).
[80] R.A. Goldbeck, S. Bhaskaran, C. Ortega, J.K. Mendoza, J.S. Olson, J. Soman, D.S. LKlinger, R.M. Esquerra. *Proc. Natl. Acad. Sci. USA*, **103**, 1254 (2006).
[81] J.C. Olson, G.N. Phillips. *J. Biol. Inorg. Chem.*, **2**, 544 (1997).
[82] B.A. Springer, K.D. Egeberg, S.G. Slighar, R.J. Rohlfs, A.J. Matthews, J.C. Olson. *J. Biol. Chem.*, **264**, 3057 (1989).
[83] M. Jaworska. *Chem. Phys.*, **332**, 203 (2007).
[84] W.R. Scheidt, M.E. Frisse. *J. Am. Chem. Soc.*, **97**, 17 (1975).
[85] T.Q. Nguen, M.C.S. Escano, N. Shimoji, H. Nakanishi, H. Kasai. *Surf. Interface Anal.*, **40**, 1082 (2008).
[86] T.Q. Nguen, M.C.S. Escano, R. Tanako, H. Nakanishi, H. Kasai. *J. Phys. Soc. Jpn.*, **78**, 014706 (2009).
[87] O. Chen, S. Groh, A. Liechty, D.P. Ridge. *J. Am. Chem. Soc.*, **121**, 11910 (1999).
[88] M.K. Ellison, W.R. Scheidt. *Inorg. Chem.*, **37**, 382 (1998).
[89] X.-Q. Zhu, Q. Li, Q.-F. Hao, J.-P. Cheng. *J. Am. Chem. Soc.*, **124** (2002).
[90] K. Andersson, B.O. Roos. *Chem. Phys. Lett.*, **191**, 507 (1992).
[91] G. Barone, A. Silvestria, B.O. Roos. *Phys. Chem. Chem. Phys.*, **7**, 2126 (2005).
[92] C. Selçuki, R. van Eldik, T. Clark. *Inorg. Chem.*, **43**, 2828 (2004).